



## Short communication

# High-durability titanium bipolar plate modified by electrochemical deposition of platinum for unitized regenerative fuel cell (URFC)

Ho-Young Jung, Sheng-Yang Huang, Branko N. Popov\*

Center for Electrochemical Engineering, Department of Chemical Engineering, University of South Carolina, 301 Main St., Columbia, SC 29208, USA

## ARTICLE INFO

## Article history:

Received 8 September 2009  
 Received in revised form  
 30 September 2009  
 Accepted 1 October 2009  
 Available online 9 October 2009

## Keywords:

URFC  
 Electrolyzer  
 Platinum deposition  
 Titanium  
 Bipolar plate

## ABSTRACT

The electrochemical deposition of platinum on a titanium bipolar plate (Pt/Ti) was studied for applications in a unitized regenerative fuel cell (URFC). Platinum deposition on the titanium plate was carried out in the platinum precursor solution ( $1.8 \text{ g dm}^{-3}$ ) at constant acidity (pH 1.0) and temperature ( $90^\circ\text{C}$ ). The pre-treatment of the titanium plate and the applied deposition current density were optimized to obtain uniform deposition of platinum on the titanium plate. New bipolar plates were prepared using the optimized deposition process and were used in a URFC. Electrochemical deposition of platinum on the titanium plate can effectively prohibit the formation of a passive oxide layer and corrosion on the surface of the bipolar plate, leading to lower resistance and better performance. In addition, the stability of URFC performance after the operation of the cell at 2.0V for 1 h was significantly improved by the platinum deposition on the titanium bipolar plate. This improvement was mainly due to reduced corrosion on the surface of the bipolar plate.

© 2009 Elsevier B.V. All rights reserved.

## 1. Introduction

Bipolar plates play several critical roles in the fuel cell, which include distributing fuel and coolant, managing heat and water, collecting current, separating cells, and mechanically supporting the membrane electrode assembly (MEA) [1–5]. Typically, carbon-based bipolar plates can be used for the polymer electrolyte fuel cell (PEFC) due to their chemical and thermal stability, hydrophobicity, and electrical conductivity [2–8]. However, the use of a carbon bipolar plate is restricted for their application in a unitized regenerative fuel cell (URFC) due to the higher potential operation ( $>1.5 \text{ V}$ ) in the electrolyzer mode. Specifically, the carbon bipolar plate shows severe corrosion on the contact area between the carbon bipolar plate and the electrode at the extreme end of potential range [9]. This significant corrosion on the carbon bipolar plate causes a high contact resistance and poor cell performance.

In order to avoid the carbon corrosion on the bipolar plate, some materials such as stainless steel, aluminum, and titanium have been investigated as alternative materials [4,7,10–15]. Among them, titanium is a highly promising material because it provides high corrosion resistance, good mechanical strength, and titanium ions are not too poisonous for catalysts and membranes [17]. However, these metal bipolar plates also show gradual surface corrosion in the highly acidic environment of fuel cell operation. The corrosion finally causes the formation of a passive oxide layer on the

surface of metal during fuel cell operation [1–7,15–20]. The formation of this layer leads to an increase in contact resistance and a decrease in cell performance. Thus, in order to avoid the surface corrosion and the formation of a passive oxide layer for the reasonable stability of URFC performance, several methods, i.e., composites, sputtering, and other deposition techniques are investigated [3,9,12–15,21]. Among those, the deposition techniques are those considered in this study. Electro-deposition is a relatively simple technique, and adhesion of metal ions on the substrate could be optimized with the substrate metal type, surface pre-treatment, and deposition conditions.

The URFC devices have specific applications for space exploration [22]. In order to evaluate the feasibility of URFC components such as bifunctional oxygen cathode and gas diffusion layer, it is necessary to use high stability bipolar plates. The main objective of this work is to provide the metal bipolar plate with high-durability and good performance for long-term operation of a URFC. Platinum was deposited on the titanium substrate (Pt/Ti) to protect Ti from corrosion and from the formation of oxide layers. The performance and the stability of the fuel cell with the platinum-deposited titanium plate were studied under URFCs conditions.

## 2. Experimental

### 2.1. Chemical and materials

Oxalic acid (98%), concentrated sulfuric acid solution (96.7%), and the platinum precursor material (platinum chloride, 99.99%) were purchased from Sigma–Aldrich. Titanium blocks (98.9%

\* Corresponding author. Tel.: +1 803 777 7314; fax: +1 803 777 8265.  
 E-mail address: [popov@cec.sc.edu](mailto:popov@cec.sc.edu) (B.N. Popov).

**Table 1**  
Electro-deposition conditions, Pt particle sizes, and electrical conductivity of titanium substrate after the platinum deposition.

Current density (mA cm <sup>-2</sup> )	$T_{de}$ (min)	Particle size of Pt (nm)	Thickness of coating layer ( $\mu$ m)	Surface composition of plate (%)		Electrical conductivity (S cm <sup>-1</sup> )
				Pt	Ti	
0	0	0	0	0	100	54
1	178.6	9.0	0.57	33.1	66.9	65
5	35.3	10.9	0.98	71.7	28.3	105
10	17.7	13.2	1.21	70.6	29.4	78
50	3.5	15.1	1.27	70.1	29.9	58

purity, 7.5 cm  $\times$  7.5 cm  $\times$  1.2 cm) were machined as the bipolar plates. The bipolar plates were designed to form serpentine type of flow-fields with a surface area of 5 cm<sup>2</sup>. The depth and width of the channel in the flow-field were both 1 mm.

## 2.2. Surface pre-treatment of titanium plate

The titanium plate was physically polished with sand paper (Silicon carbide grinding paper #2400) with a grinder (Phoenix Alpha grinder, BUEHLER) and then again polished with alumina (0.05  $\mu$ m, Gamma Micropolish II) on rubbing fur. Then, the titanium plate was immersed in an oxalic acid solution (15%) at 90 °C for 5 h, and in concentrated sulfuric acid (96%) at 90 °C for 1 min. Finally, the titanium plate was washed several times in hot de-ionized water.

## 2.3. Deposition of platinum on titanium plate using electrochemical deposition process

The electrochemical deposition experiments were carried out in a plating bath (2 L) using a platinum mesh counter electrode, a Hg/HgCl reference electrode, a titanium plate working electrode and a power supply (Potentiostat/Galvanostat EG&G Princeton Applied Research, Model 273A). The liquid level of the platinum precursor solution in the plating bath was tightly set at the height of the titanium plate. The concentration of the platinum precursor solution was constantly controlled to be 1.8 g dm<sup>-3</sup>. The temperature and pH of the platinum precursor solution were controlled to remain at 90 °C and below pH 1 during the deposition process. After the set-up for the deposition process in the platinum precursor solution, a constant current was applied to the titanium plate for a constant time, as shown in Table 1. After the completion of the electrochemical deposition, the platinum-deposited titanium plate was immersed in hot de-ionized water for 6 h. Next, the temperature of the beaker was cooled down to room temperature. Finally, the platinum-deposited titanium plate was pulled out and dried.

## 2.4. Characterization studies

The platinum-deposited titanium bipolar plates were characterized by X-ray diffraction (XRD), X-ray fluorescence (XRF, Fischer, Model XDAL), and scanning electron microscope (SEM). The particle size of the platinum on the titanium plate was identified by XRD using a Rigaku D/max-rc (12 kW) equipped with a rotating Cu anode. The surface composition and the coating thickness on the titanium plate were confirmed by the XRF measurement. The surface morphology and composition of each component on the titanium bipolar plate after the electrochemical deposition of platinum was investigated with an FEI Quanta 200 Environmental Scanning Electron Microscope equipped with the energy dispersive X-ray (EDX). The electrical conductivities (through-plane) of the platinum-deposited titanium plates were measured with the two-probe method [23] using a high frequency response analyzer (Solartron Instruments, Model 1287). The resistance of the platinum-deposited titanium plate was determined with high fre-

quency resistance. The electrical conductivity was calculated using the resistance, the thickness of plate and the distance between the electrodes.

## 2.5. MEA preparation and operation of URFC

Nafion 112 (Alfa Aesar) was used to prepare the MEA. A commercial E-TEK electrode (0.5 mg cm<sup>-2</sup> Pt loading) was used as the anode. The cathode consisted of unsupported PtIr black catalyst with a catalyst loading of 4 mg cm<sup>-2</sup> prepared using a brushing technique. The PtIr catalyst was made by physically mixing platinum black (Johnson Matthey) and iridium black (Johnson Matthey) in an 85 wt%/15 wt% ratio, and then applying the gas diffusion layer (GDL). The Nafion content in the catalyst layer was 20 wt%. The electrodes and the membrane were assembled by hot-pressing at 140 °C and 800 psi for 3 min.

The URFC performance was determined by using a single cell with an electrode area of 5 cm<sup>2</sup>. The cell temperature was constantly maintained at 75 °C. In fuel cell mode, hydrogen and oxygen, humidified to 100% relative humidity (RH), were supplied to the anode and the cathode, respectively. In electrolyzer mode, de-ionized water was supplied to the bifunctional oxygen electrode. The polarization curves of the URFCs were galvanostatically measured by a power supply [9,24,25].

## 3. Results and discussion

The surface morphology of a substrate is one of the most important factors for electrochemical deposition. Fig. 1 shows the surface morphology of the Ti substrate before and after the acidic solution treatment. The bare titanium has a rough surface morphology before the acidic treatment. After the acid treatment, the titanium substrate has various types of pores and a larger surface area due to the effective corrosion of the oxalic acid and sulfuric acid solutions. Additionally, the EDX results indicated that no contaminants were found for the acid-treated titanium substrate, as shown in Fig. 2.

The surface morphology of the titanium substrate can affect the platinum deposition. Fig. 3 shows the adhesion of platinum to the titanium substrate with and without the acidic solution treatment. Without this treatment, the platinum shows poor adhesion to the titanium surface due to the lower surface area and the lower surface energy. The platinum deposited onto the titanium substrate without any acidic treatment can be easily removed by physical rubbing. On the other hand, the platinum deposited on the titanium with etching treatment showed good adhesion, even when the substrate was scrubbed or physically bent. Thus, it is found that the surface morphology and pre-treatment technique of the titanium substrate is very important for the adhesion of electro-deposited platinum onto the titanium plate.

Fig. 4 shows images of the titanium substrates after the platinum deposition at different current densities. The titanium substrates show a change of color with increasing current density due to the dense accumulation of nano-sized platinum on the titanium surface. In addition, the XRD results reveal an increase in platinum

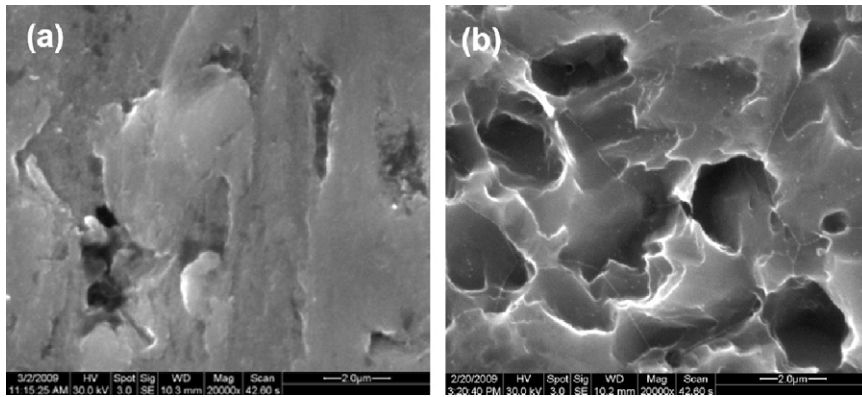


Fig. 1. The surface morphology of a bare titanium substrate (a) before and (b) after the treatment in the acidic solution.

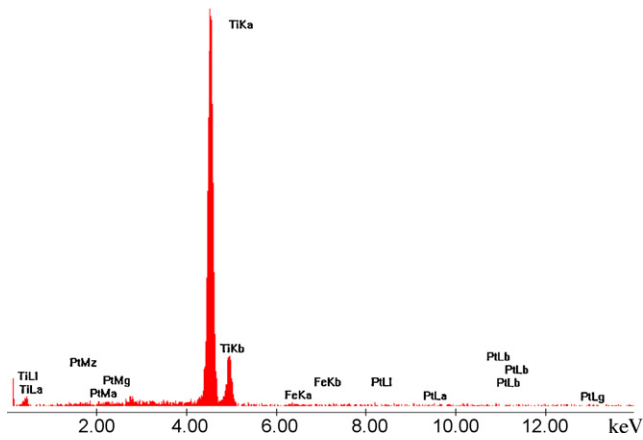


Fig. 2. Elemental analysis using EDX after the acidic treatment of the titanium substrate.

crystalline size with the increase of applied current density to the titanium plate, as shown in Table 1. In order to obtain the same platinum coating thickness, the duration of the electrochemical deposition ( $T_{de}$ ) was changed for each different current density. The thickness of the platinum layer on the titanium substrate increased with increasing current density. The observed results are probably due to a different deposition rate of platinum onto the titanium substrate and a different mechanism of platinum particle nucleation and growth at different current densities.

By increasing the applied current density on the titanium substrate, the metal composition on the surface saturated with a ratio of 70:30 in Pt:Ti components, as shown in Table 1. Additionally, the resistance changed with the increase in applied current density on the titanium substrate. In other words, the electrical conductivity of each titanium substrate after the electrochemical deposition of platinum increased with increasing current density.

Fig. 5 shows the surface morphology of the titanium substrate after the electrochemical deposition of platinum. The Pt/Ti with a current density of  $1 \text{ mA cm}^{-2}$  shows the different platinum particle sizes and shapes with other samples. The Pt particle size in the titanium substrate with a current density of  $1 \text{ mA cm}^{-2}$  is

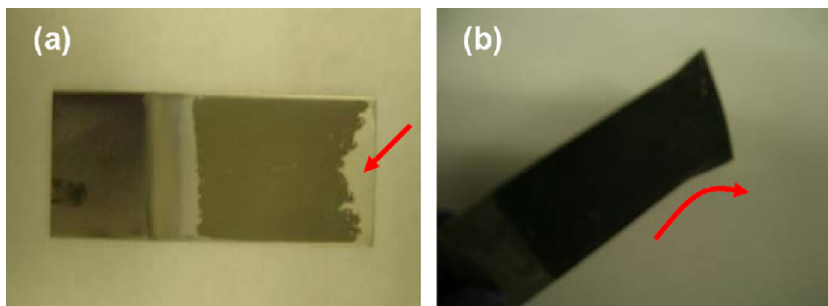


Fig. 3. The adhesion of platinum onto the titanium substrate (a) without and (b) with acidic treatment (The electrochemical deposition was carried out in the Pt precursor solution with a  $50 \text{ mA cm}^{-2}$  of current density.).

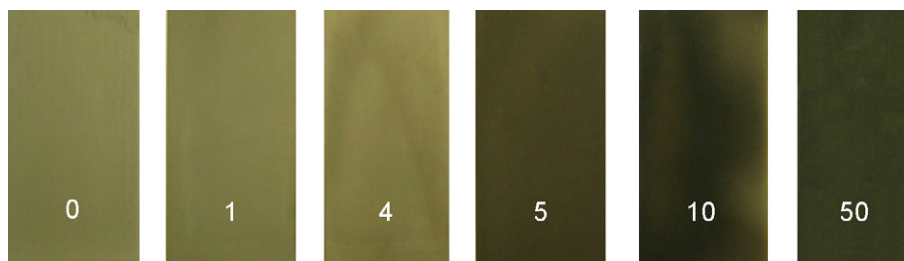
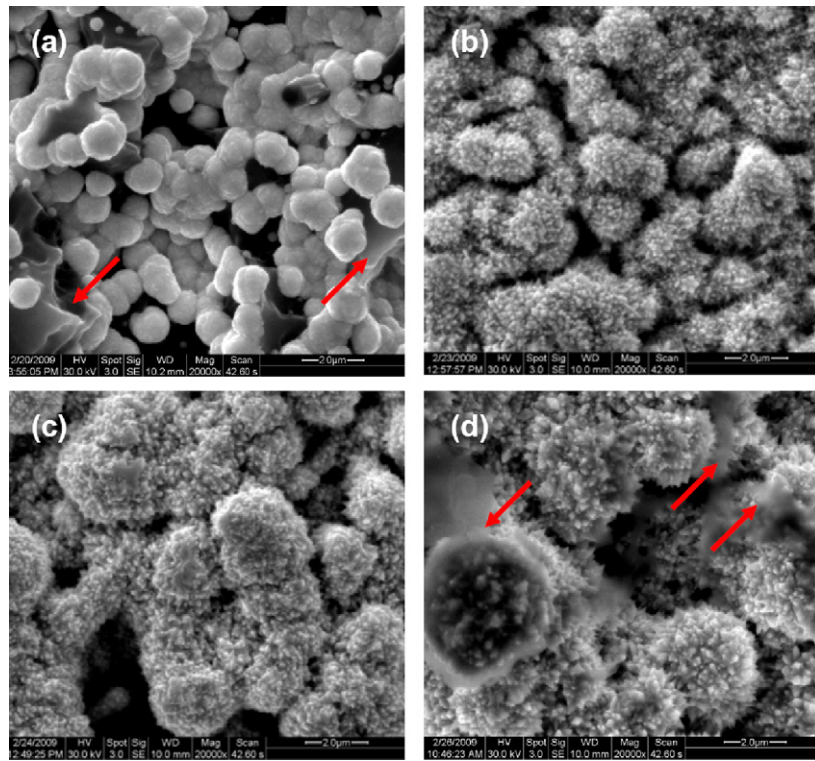


Fig. 4. The change of color in the titanium plate with increasing current density [The number is the applied current density ( $\text{mA cm}^{-2}$ ) during the electrochemical deposition process of platinum onto the titanium substrate.].





**Fig. 5.** The surface morphology of the titanium substrate after the electrochemical deposition of platinum with various current densities of (a)  $1 \text{ mA cm}^{-2}$ , (b)  $5 \text{ mA cm}^{-2}$ , (c)  $10 \text{ mA cm}^{-2}$ , and (d)  $50 \text{ mA cm}^{-2}$  (The red arrows point out the exposed titanium surface.). (For interpretation of the references to color in this figure legend, the reader is referred to the web version of the article.)

approximately  $1 \mu\text{m}$  and the platinum particles have the smooth surface and have a round, ball shape. On the other hand, the platinum particle size of Pt/Ti increases to over  $2 \mu\text{m}$  with current densities of  $5, 10, 50 \text{ mA cm}^{-2}$  and numerous nano-sized platinum

particles are newly grown on the surface of pre-existing platinum particles. Specifically, the Pt/Ti with lower and higher current densities, such as  $1$  and  $50 \text{ mA cm}^{-2}$ , are not completely covered by the platinum. This result indicates that the titanium surface is locally

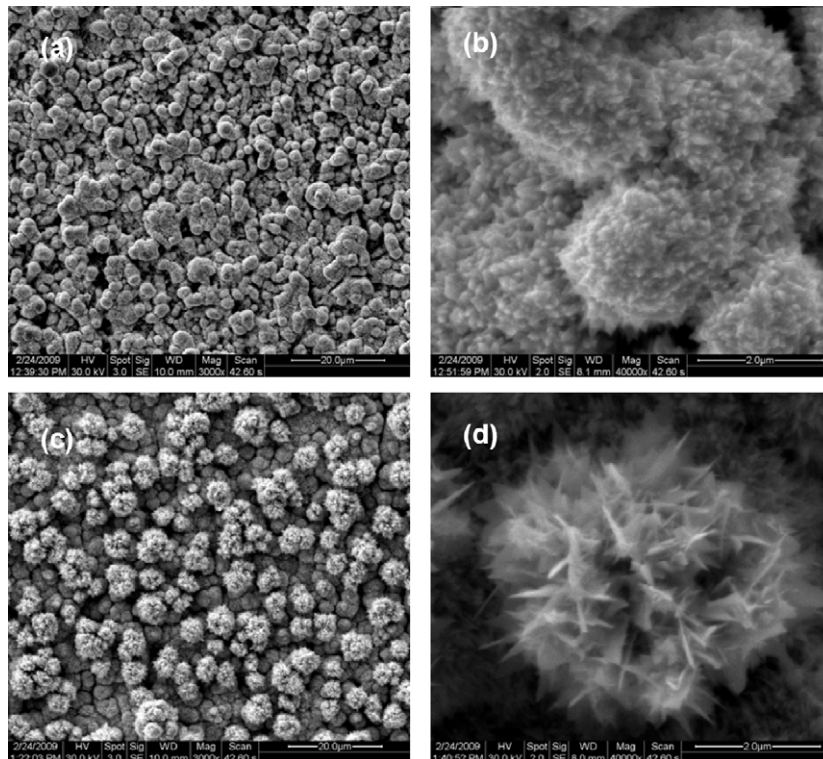


**Fig. 6.** The surface morphology of the titanium substrate with a different  $T_{de}$  of platinum.  $T_{de} = 35.3 \text{ min}$  for (a) and (b);  $106 \text{ min}$  for (c) and (d). Specifically, (b) and (d) are the enlarged scale of (a) and (c) after the electrochemical deposition of platinum.

exposed, and this exposure affects the electrical conductivity of the titanium plate. Thus, it is found that the electrical conductivity of the titanium substrate after the electrochemical deposition of platinum with the current density of  $50 \text{ mA cm}^{-2}$  is lower than that of others due to the exposed titanium. Additionally, the current density of  $5 \text{ mA cm}^{-2}$  is an optimum value for compact and good surface morphology, and higher electrical conductivity of the titanium substrate. Therefore, the applied current density to the titanium substrate is one of the factors that affect the properties of the Pt coating. Fig. 6 shows the effect of the duration of electrochemical deposition of platinum onto the titanium substrate. Figs. 6(a) and (b) shows the surface morphology of the Pt/Ti with a platinum deposition time ( $T_{\text{de}}$ ) of 35.3 min. Micro-sized platinum particles are uniformly deposited on the titanium substrate with  $T_{\text{de}} = 35.3 \text{ min}$  in Fig. 6(a). Additionally, numerous nano-sized platinum particles are grown again on the pre-existing micro-sized platinum particles in the enlarged SEM photo, as shown in Fig. 6(b). These platinum particles have a size of around 100 nm and are tetrahedron-shaped.

Figs. 6(c) and (d) shows the surface morphology of the Pt/Ti with a  $T_{\text{de}}$  of 106 min. As shown in Fig. 6(c), micro-sized platinum particles are uniformly deposited on the bottom line of the titanium substrate. However, new micro-sized platinum agglomerates bloomed on the surface of the pre-deposited titanium substrate. In addition, as shown in Fig. 6(d), platinum is grown on the bloomed micro-sized platinum particles from the nucleation point, which is shown by the needle shapes in the enlarged SEM photo. Therefore, it is clear that the platinum morphology is sufficient with a  $T_{\text{de}}$  of 35.3 min. A longer platinum deposition time affects the surface morphology and makes a needle type of platinum particle. It is anticipated that the needle type of growth in the platinum particles may become an issue for the stability of the membrane at the edge of the membrane electrode assembly (MEA) due to penetration of the membrane. Thus, it is certain that a longer duration is not effective for the deposition of platinum from the view point of surface morphology and cost issues.

The pre-treatment of the substrate, the applied current density, and the duration are the important factors for the electrochemical deposition of platinum on titanium substrates. The acidity, the concentration, and the temperature control of the platinum precursor solution are also important factors for the preparation of platinum-deposited titanium bipolar plates. They affect the deposition process and the surface morphology of the platinum-deposited titanium substrate. In order to obtain good surface morphology and high bipolar plate performance, in this study the acidity of the platinum precursor solution was controlled with a pH meter to be below a pH of 1. The concentration of the platinum precursor solution was constantly controlled to be  $1.8 \text{ g dm}^{-3}$  during the electro-deposition process. Additionally, the temperature of the platinum precursor solution was controlled to remain at  $90^\circ\text{C}$ . This value was optimized for good adhesion of platinum particles onto the titanium substrate through several iterations of trial and error. With these conditions for the electrochemical deposition of platinum, we prepared the new platinum-deposited titanium bipolar plates for the operation of URFC.

Fig. 7 shows the initial performance of the unit cell of the URFC in both fuel cell mode and electrolyzer mode with the titanium bipolar plates before and after the platinum deposition. As shown in Fig. 7(a), the performance of the unit cell significantly increased in fuel cell mode. This increase in performance is due to the decrease in the ohmic resistance after platinum deposition on the titanium bipolar plate. The ohmic resistances of the cell with titanium bipolar plates before and after the electrochemical deposition of platinum were  $0.39$  and  $0.15 \Omega$ , respectively. The significant decrease of ohmic resistance results from the electrochemical deposition of platinum on the titanium bipolar plate, because the other com-

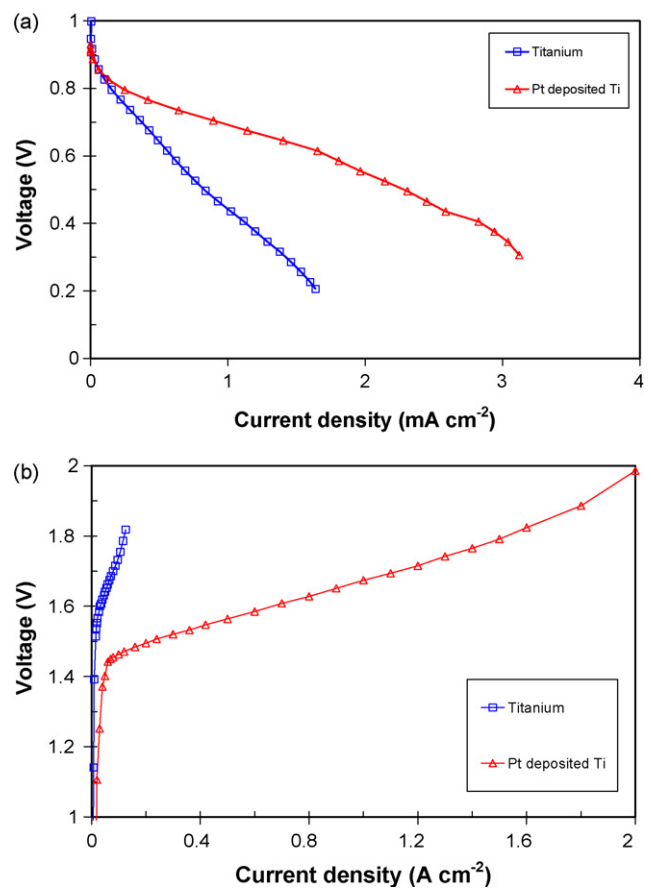


Fig. 7. The initial performance of unit cell in both (a) fuel cell mode and (b) electrolyzer mode of URFC with the Ti and Pt/Ti bipolar plates.

ponents in the MEA are almost the same. This finding means that electrochemical deposition of platinum on the titanium bipolar plate can effectively suppress the formation of a passive oxide layer [9], resulting in high cell performance. As shown in Fig. 7(b), similar results were obtained in electrolyzer mode. In other words, the increase of potential in electrolyzer mode was highly suppressed with the Pt/Ti bipolar plate due to the decrease of ohmic resistance, leading to a good cell performance. Furthermore, Table 2 shows the ohmic resistances of the cell with different types of bipolar plates. The ohmic resistances of the cell with titanium bipolar plates before and after corrosion test were  $0.39$  and  $0.45 \Omega$ , respectively. These results indicated that electro-deposition of platinum on the titanium bipolar plate can effectively suppress the passive oxide layer formation, resulting in high URFC performance.

The problem with using a carbon-based bipolar plate is the significant corrosion on the surface of the carbon bipolar plate [9]. This corrosion leads to increased ohmic resistance and decreased cell performance after the operation of unit cell at high potential, such as  $2.0 \text{ V}$  for  $1 \text{ h}$ . However, the titanium-based bipolar plate after the electrochemical deposition of platinum does not show any corrosion on the surface of the platinum-deposited titanium bipolar plate. Additionally, as shown in Table 2, the carbon-based bipolar plate showed a significant difference in the cell resistance before and after the operation of the unit cell at  $2.0 \text{ V}$  for  $1 \text{ h}$  due to the severe corrosion of the carbon bipolar plate. In other words, the resistance difference in the unit cell with the carbon-based bipolar plate mainly comes from the increased contact resistance between the MEA and the corroded carbon-based bipolar plate, in addition to the degradation of the GDL in the MEA. The titanium-based bipolar plate after the electro-deposition of platinum showed a relatively

**Table 2**

Ohmic resistance of cell with difference types of bipolar plates after the operation of unit cell at 2.0 V for 1 h.

Corrosion test of bipolar plate (operation of unit cell at 2.0 V for 1 h)	Resistance ( $\Omega$ )	
	Before corrosion test	After corrosion test
Carbon-based bipolar plate	0.15	1.24
Titanium-based bipolar plate	0.39	0.45 <sup>a</sup>
Pt/Ti bipolar plate	0.15	0.17

<sup>a</sup> The resistance increase rate is  $0.06 \Omega \text{ h}^{-1}$ .

small difference in the cell resistance before and after the operation of unit cell at 2.0 V for 1 h. The small difference of the ohmic resistance in the unit cell with the Pt/Ti bipolar plate is probably due to the degradation of the GDL, because no corrosion was observed on the Pt/Ti bipolar plate.

Fig. 8 shows the performance stability of the unit cell with different bipolar plates after the operation of the cell at 2.0 V every day. As shown in Fig. 8(a), the unit cell with carbon-based bipolar plates shows poor stability after the operation of the unit cell in harsh conditions. Aside from the corrosion of the GDL, this is mainly due to the corrosion of the carbon bipolar plate, leading to the increased contact resistance. As shown in Fig. 8(b), the unit cell with the Pt/Ti bipolar plates exhibits better stability than that with carbon-based bipolar plates after the operation of unit cell at 2.0 V for 1 h. Because there is no corrosion on the surface of Pt/Ti bipolar plate, the main reason for performance degradation in the polarization curve is probably the degradation of the GDL. In spite of the degradation of the material in the MEA at the severe condition of corrosion, the stability of unit cell performance was significantly improved by the electrochemical deposition of

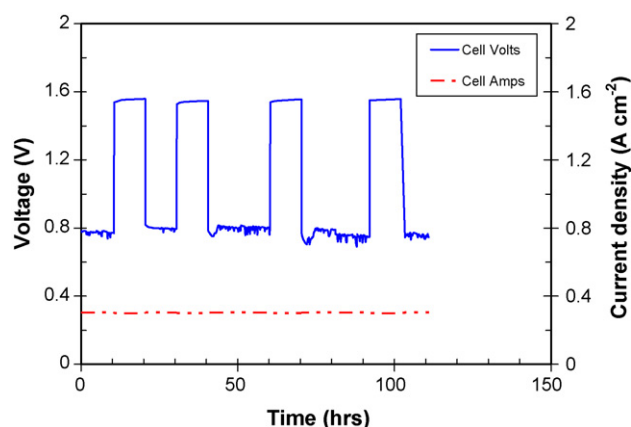


**Fig. 9.** Long-term cycling test of the URFC in both fuel cell mode and electrolyzer mode for 100 h at current density of  $300 \text{ mA cm}^{-2}$ .

platinum on the titanium bipolar plate. This improved stability is mainly due to the suppressed corrosion and formation of an oxide layer on the surface of Pt/Ti bipolar plate.

Based on the stability data of the unit cell with Pt/Ti bipolar plates in the polarization curve, a long-term cycling test of the URFC was carried out in both fuel cell and electrolyzer mode for 100 h at the current density of  $300 \text{ mA cm}^{-2}$  as shown in Fig. 9. The potentials were kept at 0.79 V and 1.58 V in fuel cell mode and electrolyzer mode, respectively. Thus, the potential stability in both fuel cell mode and electrolyzer mode is very promising for the reasonable application of URFCs using platinum-deposited titanium bipolar plates. The platinum coating is an expensive approach. However, in order to test the catalyst performance under URFC operating conditions, use of highly stable bipolar plates are mandatory.

#### 4. Conclusion

Platinum deposition on the titanium bipolar plate has been performed in a platinum precursor solution using an electrochemical deposition technique. For the optimal deposition of platinum on the titanium bipolar plate. The process parameters such as: pre-treatment of titanium plate, applied current density, duration of the platinum deposition, acidity and the concentration of the platinum precursor solution, and plating temperature were optimized in this study. The initial performance of the unit cell with newly prepared Pt/Ti bipolar plates has been significantly improved due to the suppressed formation of the passive oxide layer. The polarization studies indicated a good stability after operation of the unit cell at 2.0 V for 1 h and in the cycling test at a current density of  $300 \text{ mA cm}^{-2}$ . The deposition of platinum on titanium bipolar plates effectively inhibits the formation of the oxide layer and the corrosion on the titanium surface, leading to a decreased contact resistance and good stability for the long-term operation of URFCs.

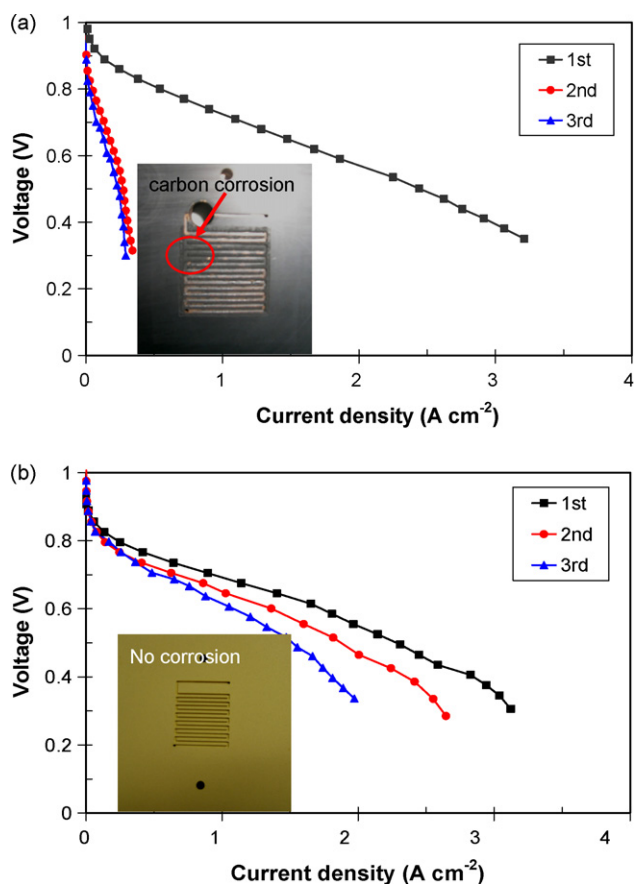


**Fig. 8.** The stability of the unit cell performance after the operation of cell at 2.0 V for 1 h every day with (a) carbon-based bipolar plate and (b) platinum-deposited titanium bipolar plate.

## Acknowledgement

The financial support of NASA-EPSCoR is gratefully acknowledged.

## References

- [1] B.K. Kakati, V. Mohan, *Fuel Cells* 8 (2008) 45.
- [2] W. Yoon, X. Huang, P. Fazzino, K.L. Reifsnider, M.A. Akkaoui, *J. Power Sources* 179 (2008) 265.
- [3] P.H. Maheshwari, R.B. Mathur, T.L. Dhami, *J. Power Sources* 173 (2007) 394.
- [4] A. Hermann, T. Chaudhuri, P. Spagnol, *Int. J. Hydrogen Energy* 30 (2005) 1297.
- [5] Y. Wang, D.O. Northwood, *J. Power Sources* 175 (2008) 40.
- [6] R.C. Makkus, A.H.H. Janssen, F.A. Bruijin, R.K.A.M. Mallant, *J. Power Sources* 86 (2000) 274.
- [7] Y.J. Ren, C.L. Zeng, *J. Power Sources* 171 (2007) 778.
- [8] C.Y. Chung, S.K. Chen, T.S. Chin, T.H. Ko, S.W. Lin, W.M. Chang, S.N. Hsiao, *J. Power Sources* 186 (2009) 393.
- [9] H.Y. Jung, S.Y. Huang, G. Prabhu, B.N. Popov, *J. Power Sources* 194 (2009) 972.
- [10] V. Mehta, J.S. Cooper, *J. Power Sources* 114 (2003) 32.
- [11] J. Pettersson, B. Ramsey, D. Harrison, *J. Power Sources* 157 (2006) 28.
- [12] P.L. Hentall, J.B. Lakeman, G.O. Mepsted, P.L. Adcock, J.M. Moore, *J. Power Sources* 80 (1999) 235.
- [13] D.P. Davies, P.L. Adcock, M. Turpin, S.J. Rowen, *J. Power Sources* 86 (2000) 237.
- [14] S.H. Wang, J. Peng, W.B. Lui, *J. Power Sources* 160 (2006) 485.
- [15] S.H. Wang, J. Peng, W.B. Lui, J.S. Zhang, *J. Power Sources* 162 (2006) 486.
- [16] A. Agneaux, M.H. Plouzenec, L. Antoni, J. Granier, *Fuel Cells* 6 (2006) 47.
- [17] Y.A. Dobrovol'skii, A.E. Ukshe, A.V. Levchenko, I.V. Arkhangel'skii, S.G. Ionov, V.V. Avdeev, S.M. Aldoshin, *Russ. J. Gen. Chem.* 77 (2007) 752.
- [18] J. Wind, R. Spah, W. Kaiser, G. Bohm, *J. Power Sources* 105 (2002) 256.
- [19] H. Tawfik, Y. Hung, D. Mahajan, *J. Power Sources* 163 (2007) 755.
- [20] D.R. Hodgson, B. May, P.L. Adcock, D.P. Davies, *J. Power Sources* 96 (2001) 233.
- [21] J. Iniesta, J.G. Garcia, J. Fernandez, V. Montiel, A. Aldaz, *J. Mater. Chem.* 9 (1999) 3141.
- [22] F. Mitlitsky, B. Myers, A.H. Weisberg, *Energy Fuels* 12 (1998) 56.
- [23] W. Vielstich, A. Lamm, H.A. Gasteiger, *Handbook of fuel cells*, vol. 3, John Wiley & Sons Ltd, 2003, pp. 526–528.
- [24] T. Ioroi, K. Yasuda, Z. Siroma, N. Fujiwara, Y. Miyazaki, *J. Power Sources* 112 (2002) 583.
- [25] G. Chen, H. Zhang, J. Cheng, Y. Ma, H. Zhong, *Electrochem. Commun.* 10 (2008) 1373.